

Kinematic Design of 3-Limb Spatial Parallel Mechanism with Two Identical Limbs for a Humanoid Robotic Shoulder Complex

C. Srikanth Rao¹, A.Naga Phaneendra², K. Kumar³, P. Pavan Kumar⁴,
Nallam Venkata Siva⁵

¹(M.Tech, Mechanical Engineering)

²(M.Tech, Mechanical Engineering)

³(B.Tech, Mechanical Engineering)

⁴(M.Tech, Mechanical Engineering)

⁵(B.Tech, Mechanical Engineering)

Abstract: Automation and robotics are two closely related technologies. Robotics is a form of industrial automation. An industrial robot is a reprogrammable, multifunctional manipulator designed to perform variety of tasks. In recent literatures most of the robotic shoulders incorporated spherical joints representing the function of glenohumeral articulation. The design of spherical joints is complicated and range of motions is limited. So in this project the kinematic analysis of 3-limb parallel mechanisms consisting of 2URP and 1RRP chain for the shoulder of a human robot is present. Then the kinematic properties of human shoulder are designed by using a fully parallel mechanism with three driven extendable legs connecting a fixed base and a movable platform. The main aim is to describe the design of humanoid robotic shoulder mechanism simulating the function of sternoclavicular and scapulothoracic joints. The performance indices of the manipulator (condition number, transmission index) are obtained in MATLAB software.

Keywords: Automation, robotics, glenohumeral articulation, 2URP and 1RRP, sternoclavicular and scapulothoracic joints, manipulator, MATLAB

I. Introduction

Nowadays, most of the robotic shoulders incorporate different types of universal and spherical joints to represent the function of glenohumeral articulation [1]. In humans, joints may be classified functionally based upon how much movement they allow. A joint that permits no movement is known as synarthrosis. An amphiarthrosis allows a slight amount of movement at the joint. The intervertebral disks of the spine and the pubic symphysis of the hips are the example of amphiarthrosis.

The third functional class of joint is the freely movable diarthrosis joints. Diarthroses have the highest range of motion of any joint and include the elbow, knee, shoulder and wrist.

The human shoulder is the most mobile joint in the body. This mobility provides the upper extremity with tremendous range of motion such as adduction, abduction, flexion, extension, internal rotation, external rotation and 360° circumduction in the sagittal plane. Furthermore, the shoulder allows for scapular protraction, retraction, elevation and depression. This wide range of motion also makes the shoulder joint unstable. This instability compensated for by rotator cuff muscles, tendons, ligaments and the glenoid labrum.

The Shoulder joint is the assembly of three articulations, which are the sternoclavicular joint, the scapulothoracic joint and the glenohumeral joint. The first two connect the shoulder to the body and third joint connects the upper arm to the shoulder. A number of coupled actuators will drive them. The first two joints possess relatively small ranges of motion but their contribution to the arm performances is extremely important. The shoulder complex radically increases the arms mobility and reachability by the use of sternoclavicular and scapulothoracic degree of freedom. This role of the sternoclavicular and the scapulothoracic joint in the human arm movement has been demonstrated in previous work of J. Lenarcic [2, 3]. In recent investigations they also enlarge the self-motion ability and the amount of positioning redundancy of the arm [4].

The main aim of the article is to describe the design of humanoid robotic shoulder mechanism simulating the function of the sternoclavicular and the scapulothoracic joints. In this work, the kinematic properties of human shoulders are designed by utilizing a fully parallel mechanism with three driven extendable legs connecting a fixed base and a movable platform. The base is attached to the body, while the upper arm is connected to the movable platform by a glenohumeral joint.

II. Kinematic Analysis of 3-Limb Spatial Parallel Mechanism with Two Identical Limbs Spatial Parallel Manipulator

The parallel manipulator at hand consists of a moving platform (MP) and a base platform (BP) that are connected to each other by means of four legs, as shown in Figure 1. Each leg contains two links coupled by a prismatic joint. The central leg is connected to the MP by a universal joint and fixed to the BP. The other three legs are connected to the MP by spherical joints and to the BP by universal joints. The frames XYZ and xyz are inertial and moving frames attached to the BP and MP at points O and O_M , respectively. The system has 3-DoF and three linear actuators are connected to three circumferential legs. Hence the MP has three motions: translation along the Z-axis (heave), rotation about the y-axis (pitch) and rotation about the x-axis (roll). Upon obtaining the kinematic constraint equations and the time differentiation of the equations thus obtained, we can obtain the relation between input or joint velocity, \dot{q} , and the output or Cartesian velocity, t , as follows

$$At = B\dot{q}$$

$$\dot{q} = \begin{bmatrix} q_1 & q_2 & q_3 \end{bmatrix}^T$$

$$t = \begin{bmatrix} \varphi & \psi & h \end{bmatrix}^T$$

$$A = \begin{bmatrix} a_{11} & a_{12} & a_{13} \\ a_{21} & a_{22} & a_{23} \\ a_{31} & a_{32} & a_{33} \end{bmatrix}$$

$$B = \begin{bmatrix} q_1 & 0 & 0 \\ 0 & q_2 & 0 \\ 0 & 0 & q_3 \end{bmatrix}$$

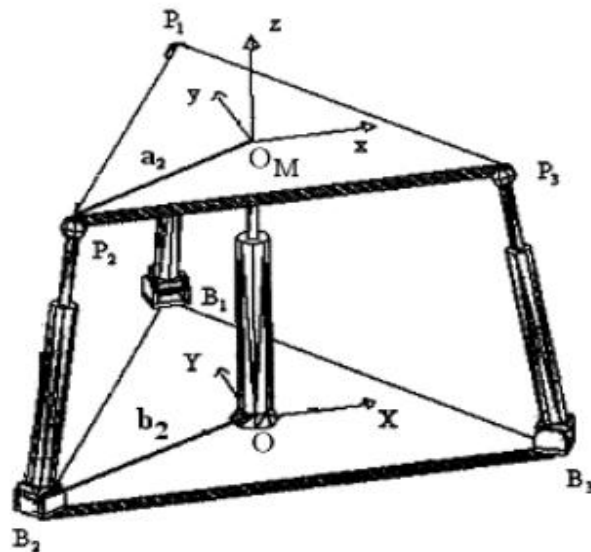


FIG 1: 3-DoF spatial parallel manipulator

A 3-limb Spatial Parallel Mechanism with two identical limbs

Inverse kinematic analysis of 3-limb Spatial Parallel Mechanism with two identical limbs:

The inverse kinematics problem involves mapping a known pose of the output platform of the mechanism to a set of input joint variables that will achieve that pose. The inverse kinematics problem of the parallel manipulator can be described in closed form.

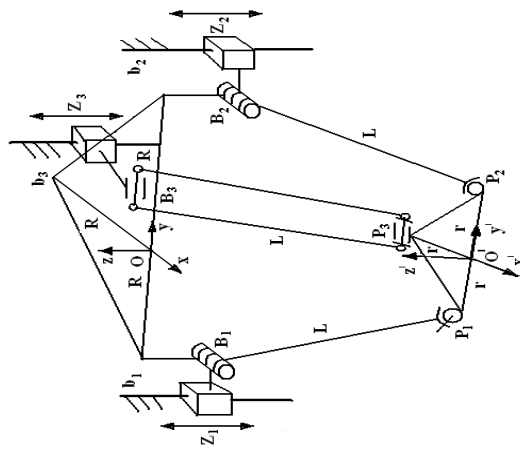


FIG 2: Kinematic model of 3-limb Spatial Parallel Mechanism with two identical limbs

A kinematic model of the manipulator is shown in Fig. 4.2. Vertices of the output platform are denoted as platform joints p_i ($i = 1, 2, 3$), and vertices of the base platform are denoted as b_i , ($i = 1, 2, 3$). A fixed global reference system $R : O - xyz$ is located at the center of the side b_1b_2 with the z axis normal to the base plate and the y axis directed along b_1b_2 . Another reference frame, called the top frame $R' : O' - x'y'z'$ is located at the center of the side P_1, P_2 . The z' axis is perpendicular to the output platform and y' axis directed along P_1, P_2 . The length of link for each leg is denoted as L , where $P_i B_i = L$, $i = 1, 2, 3$. What we should note that, in some case, the length of the link $P_3 B_3$ can be different from that of $P_1 B_1$, and $P_2 B_2$. For this analysis, the pose of the moving platform is considered known, and the position is given by the position vector $(O')_{\mathfrak{M}}$ and the orientation is given by a matrix Q .

Then there are

$$(o')_R = (xyz)^T \quad \dots\dots\dots (1)$$

where $x = 0$ and

$$Q = \begin{bmatrix} \cos \phi & 0 & \sin \phi \\ 0 & 1 & 0 \\ -\sin \phi & 0 & \cos \phi \end{bmatrix} \quad \dots\dots\dots (2)$$

where the angle ϕ is the rotational degree of freedom of the output platform with respect to y axis. The coordinate of the point P_i in the frame R' can be described by the vector $(p_i)_{R'}$ ($i = 1, 2, 3$), and

$$(p_1)_{R'} = \begin{pmatrix} 0 \\ -r \\ 0 \end{pmatrix}, (p_2)_{R'} = \begin{pmatrix} 0 \\ r \\ 0 \end{pmatrix}, (p_3)_{R'} = \begin{pmatrix} -r \\ 0 \\ 0 \end{pmatrix} \quad \dots\dots\dots (3)$$

Vectors $(b_i)_{R'}$ ($i = 1, 2, 3$) will be defined as the position vectors of base joints in frame R , and

$$(b_1)_{R'} = \begin{pmatrix} 0 \\ -R \\ Z_1 \end{pmatrix}, (b_2)_{R'} = \begin{pmatrix} 0 \\ R \\ Z_2 \end{pmatrix}, (b_3)_{R'} = \begin{pmatrix} -R \\ 0 \\ Z_3 \end{pmatrix} \quad \dots\dots\dots (4)$$

The vector ($i = 1, 2, 3$) in frame $0 - xyz$ can be written as

$$(p_i)_R = Q(p_i)_{R'} + (o')_R \quad \dots\dots\dots (5)$$

Then the inverse kinematics of the parallel manipulator can be solved by writing following constraint equation:

$$\|(p_i) - b_i\|_R = L \quad \dots\dots\dots (6)$$

(where $i=1,2,3$)

Hence, for a given manipulator and for prescribed values of the position and orientation of the platform, the required actuator inputs can be directly computed from (6). that is

$$Z_1 = \pm \sqrt{L^2 - (-r + y + R)^2} + Z \quad \dots\dots\dots (7)$$

$$Z_2 = \pm \sqrt{L^2 - (r + y - R)^2} + Z \quad \dots\dots\dots (8)$$

$$Z_3 = \pm \sqrt{L^2 - (r \cos \phi + R)^2 - y^2} + r \sin \phi + Z \quad \dots\dots\dots (9)$$

From (7)-(9), we can see that there are eight inverse kinematics solutions for a given pose of the parallel manipulator.

Jacobian analysis of Parallel Manipulators

The Jacobian analysis of parallel manipulators is a much more difficult problem than that of serial manipulators because there are many links that form a number of closed loops. An important limitation of parallel manipulator is that singular configurations may exist within its work space where the manipulator gains one or more degrees of freedom and therefore loses its stiffness completely. The Jacobian matrix is converted into two matrices: one associated with the direct kinematics and the other with the inverse kinematics. Depending on which matrix is singular, a closed-loop mechanism may be at a direct kinematic singular configuration, an inverse kinematic singular configuration, or both.

A parallel manipulator is one which consists of a moving platform and a fixed base connected by several limbs. The moving platform serves as the end effector. Because of the closed-loop construction, some of the joints can be controlled independently and the other joints are passive. Generally, the number of actuated joints should be equal to the number of degrees of freedom of the manipulator.

Let the actuated joint variables be denoted by a vector \mathbf{q} and the location of the moving platform be described by a vector \mathbf{x} . Then the kinematic constraints imposed by the limbs can be written in the general form.

$$\mathbf{F}(\mathbf{x}, \mathbf{q}) = 0, \quad \dots\dots\dots (10)$$

Differentiating Eq. (7) with respect to time, the following relationship between the input joint rates and end-effector output velocity can be written as

$$\dot{\mathbf{J}}_x \dot{\mathbf{x}} = \dot{\mathbf{J}}_q \dot{\mathbf{q}} \quad \dots\dots\dots (11)$$

Where

$$\mathbf{J}_x = \frac{\partial \mathbf{F}}{\partial \mathbf{x}} \quad \text{and} \quad \mathbf{J}_q = \frac{\partial \mathbf{F}}{\partial \mathbf{q}} \quad \dots\dots\dots (12)$$

The derivation above leads to two separate Jacobian matrices. Hence the overall Jacobian matrix, \mathbf{J} , can be written as

$$\dot{\mathbf{q}} = \mathbf{J} \dot{\mathbf{x}} \quad \dots\dots\dots (13)$$

Where $\mathbf{J} = \mathbf{J}_q^{-1} \mathbf{J}_x$. We note that the Jacobian matrix defined in Eq. (3) for a parallel manipulator corresponds to the inverse Jacobian of a serial manipulator.

Jacobian matrix of 2URP and 1RRP manipulator is obtained by differentiating Eq. (6).

$$\mathbf{J} = \mathbf{j}_q^{-1} \mathbf{j}_x = \mathbf{B}^{-1} \mathbf{A} \quad \dots\dots\dots (14)$$

$$\mathbf{A} = \begin{bmatrix} z - z_1 & 0 & 0 \\ 0 & z - z_2 & 0 \\ 0 & 0 & r \sin \phi + z - z_3 \end{bmatrix} \quad \dots\dots\dots (15)$$

$$\mathbf{B} = \begin{bmatrix} -r + y + R & z - z_1 & 0 \\ r + y - R & z - z_2 & 0 \\ y & r \sin \phi + z - z_3 & R r \sin \phi + r(z - z_3) \cos \phi \end{bmatrix} \quad \dots\dots\dots (16)$$

Performance indices of 3-limb spatial Parallel Manipulator:

The three performance indices namely condition number, manipulability and minimum singular value are evaluated for the 3-limb Spatial Parallel Mechanism with two identical limbs. All the three indices are the functions of the Jacobian matrix.

III. Results and Discussion

Results

1. Condition Number

Table 1. Condition Number values of case: 1 and case: 2 postures.

r = 2, R = 1, L = 4	r = 3, R = 1, L = 6
0.175588	0.264732
0.178529	0.268409
0.180854	0.286684
0.182442	0.290243
0.183198	0.293734
0.183073	0.297136
0.182063	0.300422
0.142438	0.303566
0.146887	0.306533
0.151331	0.309289
0.155744	0.311794
0.160089	0.272089
0.164320	0.275766
0.168372	0.279432
0.172162	0.283075

Table 2. Condition Number values of case: 3 and case: 4 postures.

r = 2, R = 1, L = 10	r = 3, R = 1, L = 6
0.192654	0.264732
0.221147	0.275766
0.226899	0.309289
0.232589	0.311794
0.238143	0.279432
0.203922	0.283075
0.209633	0.286684
0.215382	0.290243
0.248346	0.293734
0.252593	0.297136
0.255881	0.300422
0.257856	0.303566
0.238143	0.268409
0.243450	0.272089
0.258209	0.306533

2. Transmission Index

Table 3. Transmission Index values of case: 1 and case: 2 postures.

r = 4, R = 1, L = 8	r = 5, R = 1, L = 10
0.298435	0.276660
0.300906	0.278464
0.303360	0.280276
0.305792	0.282093
0.308197	0.294875
0.310568	0.296692
0.312898	0.298502
0.315180	0.300302
0.283481	0.302089
0.285973	0.283914
0.288469	0.285740
0.290966	0.287567
0.293461	0.289396
0.295952	0.291225
0.317406	0.29305

Table 4. Transmission Index of case: 3 and case: 4 postures.

r = 4, R = 1, L = 8	r = 5, R = 1, L = 10
0.283481	0.293052
0.290966	0.294875
0.293461	0.296692
0.295952	0.298502
0.298435	0.300302
0.285973	0.302089
0.300906	0.280276
0.303360	0.282093
0.305792	0.283914
0.308197	0.285740
0.310568	0.287567
0.312898	0.276660
0.315180	0.278464
0.317406	0.289396
0.288469	0.291225

Graphs

1. Condition Number

$r = 2, R = 1, L = 4$

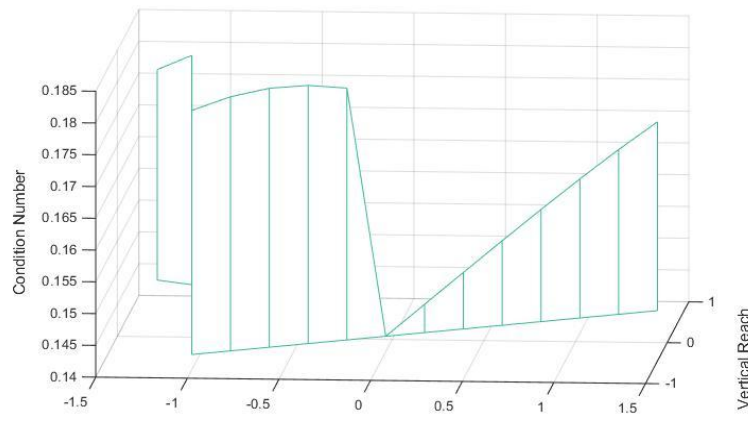


Fig 3. Condition Number of case: 1

$r = 3, R = 1, L = 6$

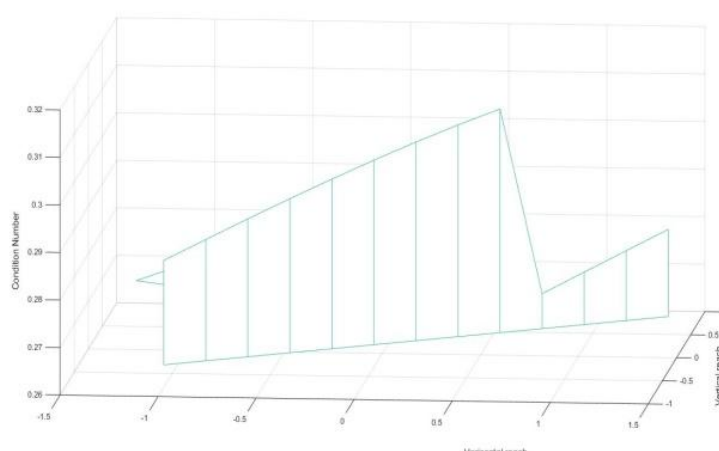


Fig 4. Condition Number of case: 2

$r = 4, R = 1, L = 8$

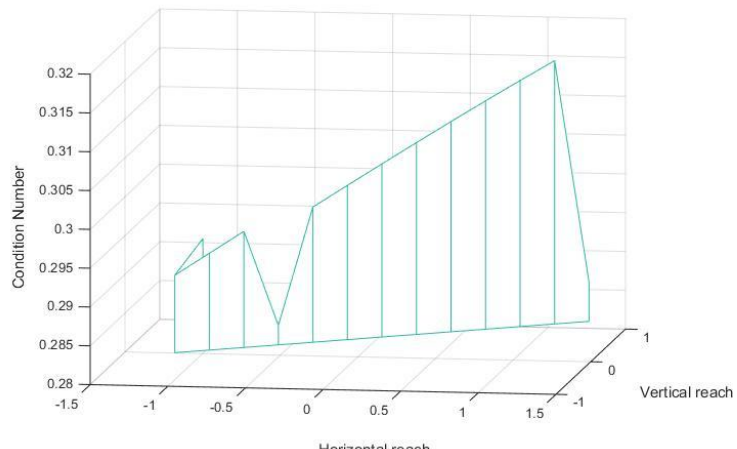


Fig 5. Condition Number of case: 3

$r = 5, R = 1, L = 10$

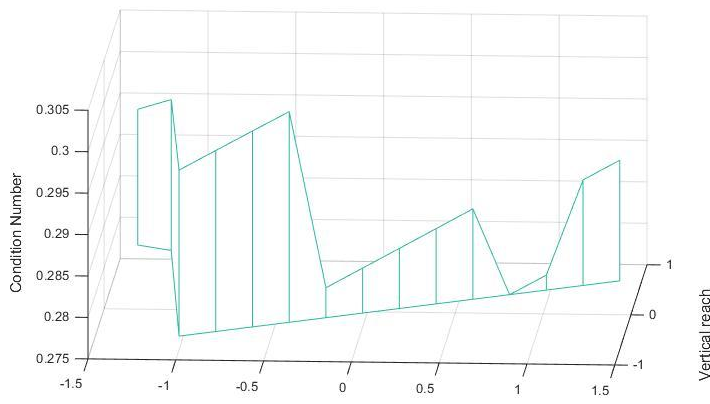


Fig 6. Condition Number of case: 4

2. Transmission Index

$r = 2, R = 1, L = 10$

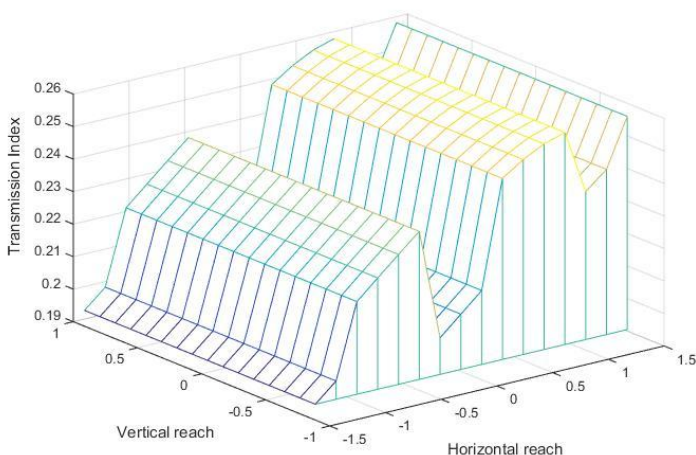


Fig 7. Transmission Index Value of case: 1

$r = 3, R = 1, L = 6$

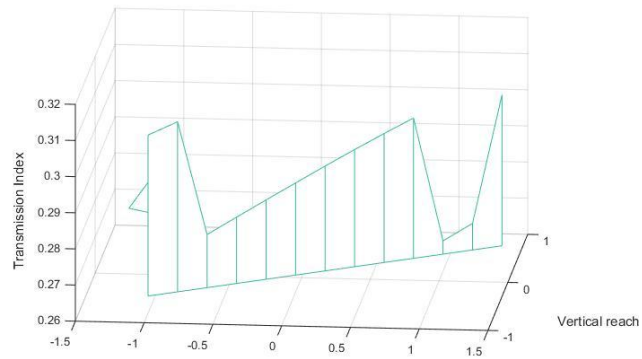


Fig 8. Transmission Index Value of case: 2

$r = 4, R = 1, L = 8$

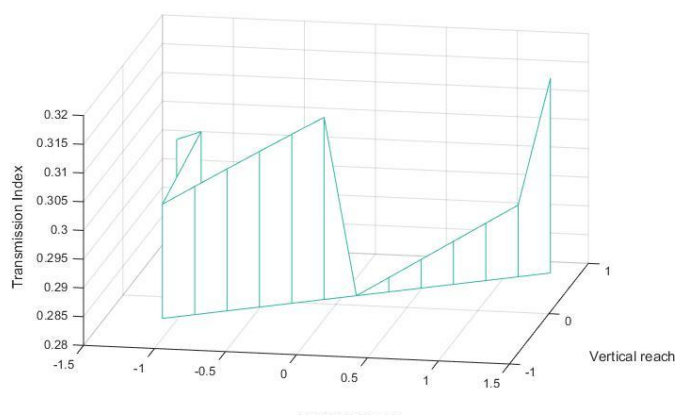


Fig 9. Transmission Index Value of case: 3

$r = 5, R = 1, L = 10$

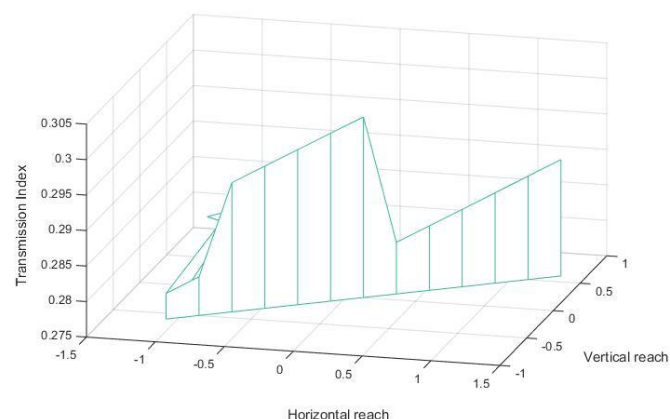


Fig 10. Transmission Index Value of case: 4

IV. Discussion

Condition Number

Case 1:

For the corresponding manipulator the link ratios' are $L_1 = L_2 = L_3 = 4$, the moving plate lengths are $R_1 = R_2 = R_3 = 1$, and the fixed plate lengths are $r_1 = r_2 = r_3 = 2$. According to the results shown in the graph the lowest Condition number Index for this manipulator is recorded as 0.142438 and the value plotted highest is 0.183198. These values may be useful for the designer for the designing of this manipulator.

Case 2:

For the corresponding manipulator the link ratios' are $L_1 = L_2 = L_3 = 6$, the moving plate lengths are $R_1 = R_2 = R_3 = 1$, and the fixed plate lengths are $r_1 = r_2 = r_3 = 3$. According to the results shown in the graph the lowest Condition number Index for this manipulator is recorded as 0.264732 and the value plotted highest is 0.311794. These values may be useful for the designer for the designing of this manipulator.

Case 3:

For the corresponding manipulator the link ratios' are $L_1 = L_2 = L_3 = 8$, the moving plate lengths are $R_1 = R_2 = R_3 = 1$, and the fixed plate lengths are $r_1 = r_2 = r_3 = 4$. According to the results shown in the graph the lowest Condition number Index for this manipulator is recorded as 0.285973 and the value plotted highest is 0.317406. These values may be useful for the designer for the designing of this manipulator.

Case 4:

For the corresponding manipulator the link ratios' are $L_1 = L_2 = L_3 = 10$, the moving plate lengths are $R_1 = R_2 = R_3 = 1$, and the fixed plate lengths are $r_1 = r_2 = r_3 = 5$. According to the results shown in the graph the lowest Condition number Index for this manipulator is recorded as 0.276660 and the value plotted highest is 0.300302. These values may be useful for the designer for the designing of this manipulator.

Transmission Index

Case 1:

For the corresponding manipulator the link ratios' are $L_1 = L_2 = L_3 = 4$, the moving plate lengths are $R_1 = R_2 = R_3 = 1$, and the fixed plate lengths are $r_1 = r_2 = r_3 = 2$. According to the results shown in the graph the lowest Transmission Index for this manipulator is recorded as 0.192654 and the value plotted highest is 0.255881. These values may be useful for the designer for the designing of this manipulator.

Case 2:

For the corresponding manipulator the link ratios' are $L_1 = L_2 = L_3 = 6$, the moving plate lengths are $R_1 = R_2 = R_3 = 1$, and the fixed plate lengths are $r_1 = r_2 = r_3 = 3$. According to the results shown in the graph the lowest Transmission Index for this manipulator is recorded as 0.264732 and the value plotted highest is 0.311794. These values may be useful for the designer for the designing of this manipulator.

Case 3:

For the corresponding manipulator the link ratios' are $L_1 = L_2 = L_3 = 8$, the moving plate lengths are $R_1 = R_2 = R_3 = 1$, and the fixed plate lengths are $r_1 = r_2 = r_3 = 4$. According to the results shown in the graph the lowest Transmission Index for this manipulator is recorded as 0.288469 and the value plotted highest is 0.317406. These values may be useful for the designer for the designing of this manipulator.

Case 4:

For the corresponding manipulator the link ratios' are $L_1 = L_2 = L_3 = 10$, the moving plate lengths are $R_1 = R_2 = R_3 = 1$, and the fixed plate lengths are $r_1 = r_2 = r_3 = 5$. According to the results shown in the graph the lowest Transmission Index for this manipulator is recorded as 0.276660 and the value plotted highest is 0.300302. These values may be useful for the designer for the designing of this manipulator.

V. Conclusion

The objective of the present work is to identify the best manipulator posture in the entire dexterous work space for a selected architecture and to select the best architecture based on the three performance measures namely Condition number, Manipulability and Minimum singular value. The performance measures are useful for determining the manipulator geometry at the design stage and for determining the manipulator posture for performing a given task at the operation stage.

The Condition Number of a matrix is used in Numerical analysis to estimate the error generated in the solution of linear system of equations by the error on the data. When this number is applied to the Jacobian matrix, the condition number will give a measure of the accuracy of the Cartesian velocity of the end effector that is produced by the joint rates calculated from Jacobian inversion. One of the most important criteria in optimal robot design is that the robot can achieve isotropic configuration i.e configurations where the condition number of its Jacobian matrix equals one. The points where the condition number reaches its minimal value may be considered as optimal working points for a given mechanical structure of a robot.

The transmission Index formed by Jacobian shows the force manipulations and velocity manipulator. The ease of transmitting the loads from the moving platform can be determined by the optimum value. So as per the transmission Indexes Case: 3 is the best structure for force and velocity manipulations.

References

- [1]. J.Lenarcic,M.M.stanisic,V.parenti-castelli,*kinematic design of a humanoid robotic shoulder complex*.
- [2]. J.Lenarcic,A.umek,*simple model of human arm reachable workspace*,IEEE trans on syst.man&cyber.,vol.6,no4,1914,pp.1239-1246.
- [3]. J.Lenarcic,*basic kinematic characteristics of humanoid manipulators*,laboratory and automation.,vol.11,1999

Kinematic Design of 3-Limb Spatial Parallel Mechanism with Two Identical Limbs for a Humanoid ..

- [4]. A.Kacin,*measurement of the human arm self-motion* Diploma thesis(j.lenarcic,adviser),Department of Physiotherapy,the university of Ljubljana,1999,in Slovenian Lung-Wen Tsai, Robot Analysis.
- [5]. Walker M.W., Manipulator kinematics and the epsilon algebra, IEEE, J. of Robot. Automat, 1988, vol. 4, pp. 186-192
- [6]. Lee E., Mavroidis C., Merlet J.P. , Five Precision Point Synthesis of Spatial RRR Manipulators Using Interval Analysis, Transactions of the ASME, 2004 Vol. 126, pp.842-849.
- [7]. Nielsen J. Roth B. On the Kinematic Analysis of Robotic Mechanisms, The International Journal of Robotics Research, December (1999), pp. 1147-1160.
- [8]. Frank C. Park, Bobrow J.E., Efficient Geometric Algorithms for Robot Kinematic Design. ICRA 1995, pp. 2132-2137.
- [9]. Paul R.P., Robot Manipulator: Mathematics, Programming, and Control, Cambridge, MA: MIT Press, 1981, pp. 835-842.
- [10]. Dimentberg F.M., The determination of the Positions of Spatial Mechanisms, Izdatel'stvo Akademii Nauk, Moscow, 1950, pp. 212-229.
- [11]. Ravani B. and Roth B., Mappings of spatial kinematics, Trans. ASME, Journal of Mechanisms, Transmissions, (1984),460-466.